

# Development of fully-depleted and back-illuminated charge coupled devices for Soft X-ray Imager onboard the NeXT satellite

Shin-ichiro Takagi <sup>a</sup>, Takeshi Go Tsuru <sup>a</sup>, Tatsuya Inui <sup>a</sup>, Midori Ozawa <sup>a</sup>, Hironori Matsumoto <sup>a</sup>, Katsuji Koyama <sup>a</sup>, Hiroshi Tsunemi <sup>b</sup>, Emi Miyata <sup>b</sup>, Hideki Ozawa <sup>b</sup>, Daisuke Matsuura <sup>b</sup>, Masakuni Tohiguchi <sup>b</sup>, Satoshi Miyazaki <sup>c</sup>, Yukiko Kamata <sup>c</sup>, Kazuhisa Miyaguchi <sup>d</sup>, Masaharu Muramatsu <sup>d</sup>, Hisanori Suzuki <sup>d</sup>

<sup>a</sup> Department of Physics, Graduate School of Science, Kyoto University, Kitashirakawa, Sakyo-ku, Kyoto, 606-8502, Japan;

<sup>b</sup> Department of Earth and Space Science, Graduate School of Science, Osaka University, Machikaneyama-cho, Toyonaka-shi, Osaka, 560-0043, Japan;

<sup>c</sup> National Astronomical Observatory of Japan, Osawa, Mitaka, 181-8588, Japan;

<sup>d</sup> Hamamatsu Photonics K.K., 1126-1, Ichino-cho, Hamamatsu-City, 435-8558, Japan

## ABSTRACT

The *NeXT* (New X-ray Telescope) satellite to be launched around 2010, has a large effective area in the 0.1–80 keV band with the use of the multilayer super mirror (HXT). As one of the focal plane detectors for *NeXT*, we have been developing the Soft X-ray Imager (SXI). SXI consists of charge coupled devices (CCDs). In order to increase the quantum efficiency (Q.E.) as high as possible, i.e., to detect X-rays collected by HXT as many as possible, we developed a "fully-depleted and back-illuminated CCD" in the attempt to improve the Q.E. of soft X-rays by the back-illuminated structure and that of hard X-rays by thickening of a depletion layer. Thanks to a high-resistivity (over  $10\text{k}\Omega\cdot\text{cm}$ ) n-type Si, we have successfully developed Pch CCDs with very thick depletion layer of over  $300\ \mu\text{m}$ , which is 4 times thicker than that of established X-ray MOS CCDs (for example XIS, EPIC-MOS and ACIS-I). Furthermore, we have already confirmed we can thin a wafer down to  $150\ \mu\text{m}$  independent of its resistivity from the experience of the development of the back supportless CCD. Based on these successful results, we fabricated a test device of "fully-depleted and back-illuminated CCD" with the high resistivity ( $10\text{k}\Omega\cdot\text{cm}$ ) N-type Si thinned down to  $200\ \mu\text{m}$ . The pixel number and size are  $512 \times 512$  and  $24 \times 24\ \mu\text{m}$ , respectively. For optical blocking, we coated the surface with Al. We evaluated this test device and confirmed the thickness of depletion layer reaches  $200\ \mu\text{m}$  as we expected. In this paper, we present progress in development of these devices for SXI.

**Keywords:** NeXT, Soft X-ray Imager (SXI), Pch CCD, back illuminated CCD, fully depleted CCD

## 1. INTRODUCTION

The New X-ray Telescope (*NeXT*) satellite will be the next Japanese X-ray astronomical satellite following *Suzaku*, and aim to perform the imaging and spectroscopic observation in the energy band over 10 keV for the first time in the world.<sup>1</sup> Thanks to the innovation of a multilayer super mirror, *NeXT* will be able to focus the X-rays in the energy range from 0.1 keV to 80 keV (see Tawara et al. (2003)<sup>2</sup> and references therein). In particular, this super mirror maintains a high reflectivity even in the high-energy ( $> 10\ \text{keV}$ ) band. Because any satellite missions with X-ray focusing optics in the energy band above 10 keV have never been realized, *NeXT* is expected to perform the imaging and spectroscopic observation in the energy band of over 10 keV for the first time in human history. Since the non-thermal emission mainly due to the accelerated high energy particles dominates the thermal X-ray emission in the energy band above 10 keV, the observation at this band is

---

Further author information: (Send correspondence to S. Takagi)  
Shin-ichiro Takagi: E-mail: takagi9@cr.sphys.kyoto-u.ac.jp

essential to study the non-thermal X-ray emission. Therefore, the *NeXT* satellite is strongly expected to open new windows for the “non-thermal universe”.

To match the wide energy range provided by Hard X-ray telescope (HXT)<sup>3</sup> which will be onboard *NeXT*, we have been developing two different types of its focal plane detectors; (1) X-ray CCDs, which has the excellent spatial and energy resolution<sup>4,5</sup> and (2) CdTe pixelized detectors, which has the high detection efficiency for X-rays and moderate spatial resolution.<sup>6</sup> The former and the latter is named **Soft X-ray Imager (SXI)** and **Hard X-ray Imager (HXI)**, after the role to be played by each detector.

## 2. CCD FOR SOFT X-RAY IMAGER

X-ray CCD, as the focal plane detector for the X-ray astronomical missions, was firstly adopted by the *ASCA* satellites which is launched in 1993. Since then, X-ray CCD was established as one of the standard focal plane detectors and was adopted by most X-ray observatories as *Chandra*, *XMM-Newton*, and *Suzaku*. Therefore, X-ray CCD has actual results as a detector carried on the satellite. The single and, however, weakest point of CCD is the relatively low sensitivity for hard X-rays. For example, the detection efficiency of *Suzaku* XIS<sup>7</sup>, which is the one of X-ray CCDs with the highest sensitivity, is limited only to  $\sim 2\%$  at 40 keV. This is because a CCD consists of silicon which is low atomic number ( $Z$ ) matter.

In contrast, since CdTe detector consists of high- $Z$  matter, the sensitivity for the hard X-ray photons is much higher than that of a CCD. Figure 1 shows the comparison of the sensitivity between CCD (300- $\mu\text{m}$  thickness) and CdTe (0.5- and 1-mm thickness)<sup>6</sup>. Even a CdTe detector with a thickness of 0.5 mm provides good detection efficiency for the hard X-ray band up to 80 keV.

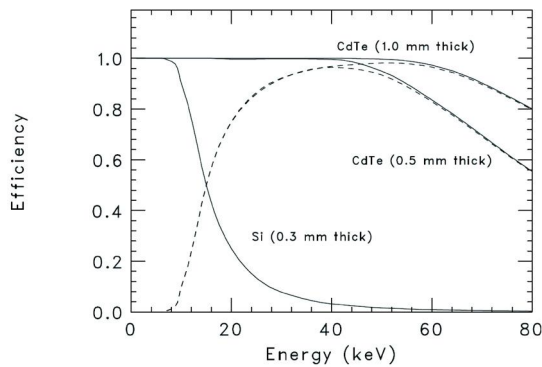


**Figure 1.** Comparison of the sensitivity between CCD (300- $\mu\text{m}$  thickness) and CdTe (0.5- and 1-mm thickness).<sup>6</sup>

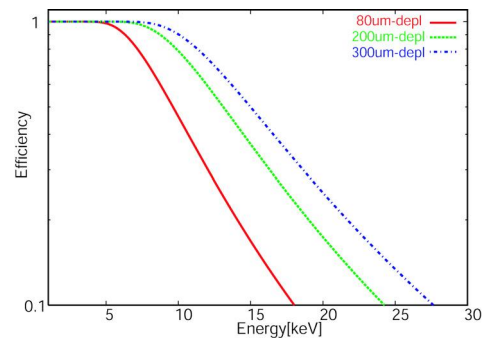


**Figure 2.** Relation between the detection efficiency and the depletion layer thickness of the CCD.

However, the position resolution of CdTe pixel detector is  $> 200 \mu\text{m}$ <sup>8</sup>, which is worse than that of X-ray CCD (10–30  $\mu\text{m}$ ) and the energy resolution for the soft X-ray ( $< 10$  keV) band is also worse. Therefore, a CCD is still suitable for the imaging and spectroscopic detector in the X-ray band below  $\sim 20$  keV. Since the non-thermal emission begins to dominate in the energy over 10 keV, the imaging and spectroscopic observation of SXI in the energy band of 10–20 keV is invaluable to explore and research the nature of non-thermal emission precisely. We need to improve the detection efficiency in the energy band over 10 keV as much as possible. The detection efficiency of CCD for X-rays of  $> 10$  keV energies strongly depend on the thickness of its depletion layer. Figure 2 shows the relation between the thickness of the depletion layer and the detection efficiency of a CCD. We can clearly see the detection efficiency for the hard X-rays of 10 keV–20 keV improves significantly by increasing the thickness of depletion layer. Therefore the thickness of the depletion layer is the key parameter for the development of SXI.

We have been developing the CCD for SXI along the “baseline plan” and “goal plan”.<sup>5</sup> The former is the conservative plan based on the successful development of high performance X-ray CCDs as CCD-CREST<sup>9</sup> and MAXI-CCD<sup>10,11</sup> which have already developed by Hamamatsu Photonics K.K. (HPK) and us. We have already

successfully fabricated the back-supportless CCD<sup>4</sup> and CCD-NeXT1,<sup>4,5,12</sup> which have the excellent spectroscopic ability and the thick depletion layer of  $\sim 80 \mu\text{m}$ .

The latter is the innovative plan to aim at the progressively high performance. We challenge to develop, however, the CCD which has the thick depletion layer of over  $200 \mu\text{m}$ . To achieve such device, we need to change the type of wafer from P-type semiconductor, which is used conventionally, to N-type one. Though this change is drastic and has the risk of failure in development, N-type semiconductor has the potential to realize the unprecedentedly thick depletion layer.

The thickness of the depletion layer ( $d_{\text{DL}}$ ) essentially depends on the mobility of the majority carrier ( $\mu$ ) and resistivity of the Si wafer ( $\rho$ ) for a given bias voltage( $V$ ) as given in the following equation,

$$d_{\text{DL}} \propto \sqrt{\mu\rho V}. \quad (1)$$

In the P-channel CCD (Pch CCD) fabricated on the N-type Si wafer, the majority carrier is an electron whose mobility is factor of three higher than that of a hole, which is majority carrier of N-channel CCD (Nch CCD). N-type silicon used for the fabrication of Pch CCD with a very high resistivity of over  $10\text{k}\Omega \cdot \text{cm}$  is available. On the other hand, the resistivity of P-type silicon used for the fabrication of Nch CCD is limited within  $\sim 5 \text{k}\Omega \cdot \text{cm}$ . The above two features allow for the operation of Pch CCD with thickness of the depletion layer of  $300\mu\text{m}$  without applying a high bias voltage.

Pch CCD was firstly fabricated by Lawrence Berkley National Laboratory (LBNL)<sup>13,14</sup>. They fabricated the back-illuminated and fully-depleted CCD on high resistivity ( $10\text{k} - 12\text{k}\Omega \cdot \text{cm}$ ) N-type wafer. They reported the thickness of depletion layer is  $\sim 300\mu\text{m}$ , which is  $\sim 4$  times thicker than that of established MOS X-ray CCDs (*Chandra* ACIS, *XMM-Newton* EPIC-MOS and *Suzaku* XIS). Furthermore, the wafer is fully depleted, in other words, no field-free layer exists. Therefore it is very easy to take the back-illuminated structure. This device acquires high sensitivity for low-energy X-rays (soft X-rays) by the back-illuminated structure and for high energy X-rays (hard X-rays) by the thick depletion layer, simultaneously.

Judging from the device fabricated by LBNL<sup>13</sup>, Pch CCD is ideal for SXI, if can be realized. However Pch CCD has no actual result as a sensor for the astronomical observation. In Japan, the group of the National Astronomical Observatory of Japan (NAOJ) is making the development of Pch CCD as a fully-depleted CCD for infrared and optical sensor<sup>15</sup> in cooperation with HPK. They are developing Pch CCD so that they will adopt it to HyperSuprime<sup>16</sup> which is one of the focal plane detectors of the *Subaru* telescope. Pch CCD is also an attractive image sensor in optical and infrared band because the thick depletion depth greatly improves the sensitivity in longer wavelength ( $> 700 \text{nm}$ ). In fact, Kamata et al. (2004)<sup>15</sup> reported the test device of Pch CCD achieved the high quantum efficiency of  $> 60\%$  at  $1 \mu\text{m}$ , which is roughly 5~6 times higher than that of ordinary CCDs.<sup>15</sup>

We adopted Pch CCD for the goal plan of SXI and participate in the development which is proceeded by NAOJ. We have already confirmed the thickness of depletion layer of test devices of Pch CCD reaches  $300 \mu\text{m}$ , which is  $\sim 4$  times thicker than that of established MOS CCDs ( $\sim 80\mu\text{m}$ )<sup>4,17</sup>. Based on the study of the back-supportless CCD for SXI,<sup>4</sup> we confirmed we can mechanically thin down the wafer to  $\sim 150 \mu\text{m}$  without any mechanical damage and performance degradation, independent of the wafer type and its resistivity. Therefore, with the use of the high resistivity N-type silicon wafer, we can expect that we can get rid of field free layer completely by thinning the wafer down to  $< 300 \mu\text{m}$  and produce the fully-depleted and back-illuminated CCD with the thick depletion layer. We successfully fabricated the test devices of Pch fully-depleted and back-illuminated CCD (BI 15-14, BI 15-22, and BI 15-06). We show the results of the performance evaluations of these devices in next section.

Furthermore, we aim to coat the surface of a CCD chip with aluminum. Because CCD is also sensitive for optical photons, the aluminum evaporation plays a role of a filter for optical blocking. This is also useful to simplify the structure of SXI because we need no longer to assemble an additional optical blocking filters. Because *Suzaku* XIS has no surface Al coating layer, it needs optical blocking filter, making the structure of XIS complicated. HPK has already successfully developed the CCD with the surface Al coating (CCD-CREST and MAXI-CCD),<sup>9-11</sup> so this goal is also considered to be very promising.

### 3. EVALUATION OF TEST MODEL OF FULLY DEVELOPED, BACK-ILLUMINATED CCD

#### 3.1. Specification

Along the goal plan, we produced the test devices of fully developed, back-illuminated CCD. We show the specification of these devices in Table 1.

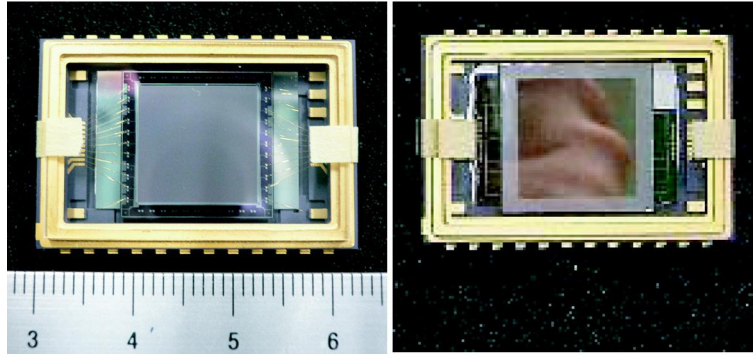


**Figure 3.** A photo of back-illuminated Pch CCD. Pixel size is  $24\mu\text{m} \times 24\mu\text{m}$  and format is  $512 \times 512$  pixels. (Left) BI 15-14 and BI 15-06. (Right) BI 15-22 . Due to Al coating, The hand of the photographer is reflected in the surface.

**Table 1.** Specification and typical performance of test models of Pch CCD (Back Illumination)

Type No.	BI 15-14	BI 15-22	BI 15-06
Format		$512 \times 512$	
Pixel size		$24 \mu\text{m} \times 24 \mu\text{m}$	
Clock phase		2 phase	
Transfer method		Full Frame Transfer	
Illuminated method		Back Illuminated	
Wafer Resistivity	$10\text{k}\Omega \cdot \text{cm}$	$10\text{k}\Omega \cdot \text{cm}$	$>10\text{k}\Omega \cdot \text{cm}$
Depletion layer	$193 \mu\text{m}$	-†	-†
Wafer*	$200 \mu\text{m}$	$200 \mu\text{m}$	$200 \mu\text{m}$
Remarks	-	Al coating	-

†: (not measured.)

\*: Nominal value reported by HPK.

These devices are fabricated on the high resistivity ( $10 \text{ k}\Omega \cdot \text{cm}$  for BI 15-14 and BI 15-22  $>10 \text{ k}\Omega \cdot \text{cm}$  for BI 15-06) N-type Si wafer and thinned down to  $200 \mu\text{m}$ . The illuminated method is the back-illuminated. Since, judging from the high resistivity of the wafer, the thickness of the depletion layer of these devices is expected to be over  $200 \mu\text{m}$ , we can expect the device is fully depleted by the thinning of the wafer down to  $\sim 200 \mu\text{m}$ . For optical blocking, we coated the surface of BI 15-22 with thin aluminum on the X-ray illumination side.

**Back bias electrode** When the depletion layer becomes thick, the distance, which the signal carrier (hole) generated in the depletion layer moves to the gate electrode, increases. Therefore, the drift time is increasing and the hole clouds spread out widely by thermal diffusion before reach the gate electrode. Because it is difficult to reconstruct the charge of the widely spread events, we need to restrain the size of the hall cloud small as much as possible. We solve this problem by installing a **back bias** electrode on the backside surface of the Pch CCD. In the case of the ordinary MOS-type CCD, the potential of the backside surface is equal to that of the substrate. By forming a back bias electrode and applying a reverse voltage (positive for Pch CCD) to it, we

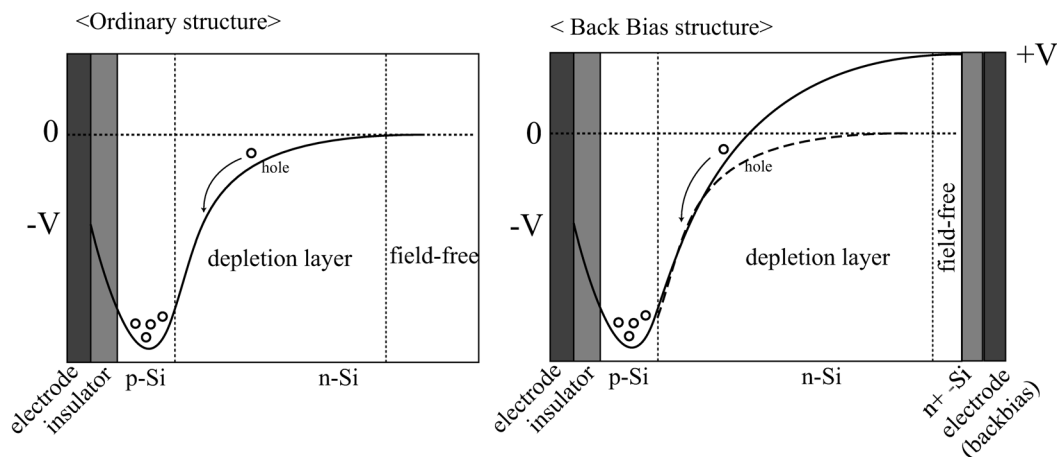


**Figure 4.** Schematic view of the potential well of the ordinary and the back bias structure.

increase the potential difference between the front and back side of a wafer. We show the schematic view of the back bias structure in Figure 4.

Then we can reduce the drift time of hole and restrain the size of the hall cloud small as a result, because the electric field in a depletion layer is intensified. Furthermore there is also another merit that we can safely apply the large potential difference which needs to make the depletion layer wider. Back bias electrode is installed on all test devices of Pch CCD described in this paper.

### 3.2. Basic characteristics

We evaluated the performance of the test device of fully-developed, back-illuminated CCD (BI 15-06). Figure 5 shows an acquired image of X-rays from  $^{109}\text{Cd}$  by BI 15-06 with the back bias voltage of 20V. We irradiated X-rays to the whole area of the CCD and successfully detected them. Table 2 shows the characteristics of BI 15-06 in various back bias voltages of 1, 5, 10, and 20V. We clearly see there are not few changes in the performance dependent on the back bias voltage. Though the readout noise of  $\sim 50 e^-$  is very high, most of which could be attributed to the noise of the readout system used in this experiment. Because the node sensitivity of this device ( $2.0\mu\text{V}/e^-$ ) is equivalent to that of Pch CCD FI 8A-IV ( $2.0\mu\text{V}/e^-$ )<sup>15</sup>, the readout noise of this test device itself is estimated to be  $\sim 10 e^-$  from the results that FI 8A-IV recorded the low readout noise of  $\sim 10 e^-$  in NAOJ<sup>15</sup>.

**Table 2.** Comparison of characteristics of BI 15-06 in various back bias voltages

$V_{\text{BB}}^\dagger$	r.o.n. <sup>‡</sup>	$S_v^{**}$	$\text{CTI}_x^b$	$\text{CTI}_y^{bb}$	$I_{\text{dark}}^\#$
[V]	[ $e^-$ ]	[ $\mu\text{V}/e^-$ ]	[ $10^{-5}$ /transfer]	[ $10^{-5}$ /transfer]	[ $e^-/\text{sec}/\text{pix}$ ]
1	51	2.0	2.1(1.9-2.4)	0.60(<1.2)	0.08
5	52	2.0	2.8(2.3-3.1)	0.84(<1.4)	0.13
10	49	2.0	2.4(2.1-2.8)	0.52(<1.1)	0.17
20	48	2.0	0.6(<1.1)	1.1 (<1.9)	0.22

Parentheses indicate the 1-sigma confidence limit.

<sup>†</sup>: Voltage applied to back bias electrode.

<sup>‡</sup>: Readout noise (r.m.s.).

<sup>\*\*</sup>: Node sensitivity.

<sup>b,bb</sup>: Charge transfer inefficiency of horizontal( $x$ ) and vertical( $y$ ) transfer.

<sup>#</sup>: Dark current at  $-98^\circ\text{C}$ .

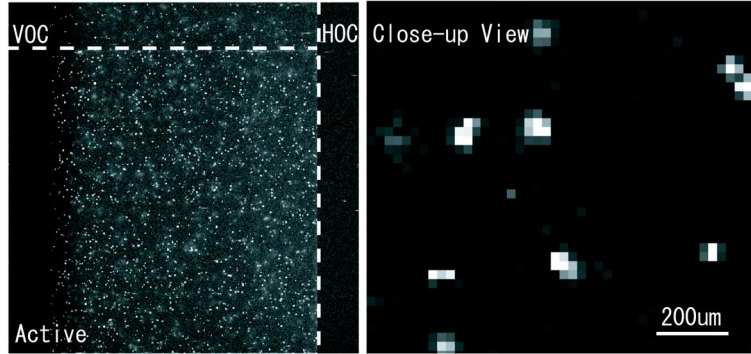


**Figure 5.** Acquired image of X-rays by BI 15-06 with the back bias voltage of 20V. (left) White dotted line shows the border between active and VOC, and HOC regions. The exposure time is 4 sec. The temperature of the CCD is  $-95^{\circ}\text{C}$  We irradiated X-ray ( $^{109}\text{Cd}$ ) to the whole area of the CCD. (right) The close-up view of detected X-ray events. Due to its thick depletion depth, back-illuminated structure, and the large energy of X-rays from  $^{109}\text{Cd}$ , many X-ray events spreads over  $2 \times 2$  pixels.

### 3.3. Thickness of depletion layer

With the well-calibrated X-ray source of  $^{109}\text{Cd}$ , we measured the detection efficiency of the BI 15-14 and the estimated the thickness of the depletion layer. As shown in Figure 6, we successfully detected the collimated X-ray events.

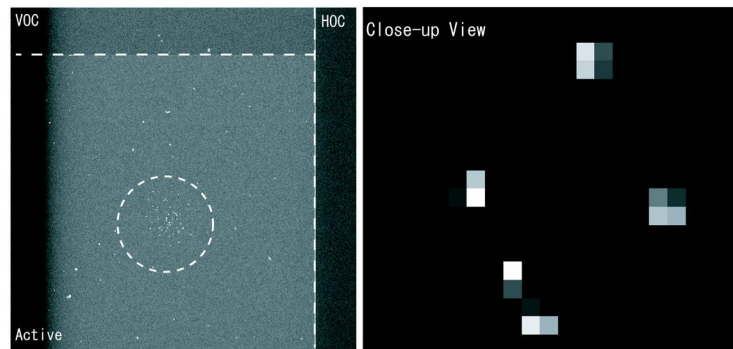


**Figure 6.** Acquired image of X-rays with Pch 15-14. The back bias voltage is 0 V. (left) White dotted line shows the border between active and VOC, and HOC regions. We irradiated the collimated X-ray ( $^{109}\text{Cd}$ ) within the white dotted circle area on this device. (right) The close up view of detected X-ray events. Due to its thick depletion depth, back-illuminated structure, and the large energy of X-rays from  $^{109}\text{Cd}$ , many X-ray events spread over  $2 \times 2$  pixels and are classified into grade 7.

Due to its thick depletion depth, back-illuminated structure, and the large energy of X-rays from  $^{109}\text{Cd}$ , many X-ray events spread over  $2 \times 2$  pixels and are classified into grade 7. In X-ray astronomy, we conventionally judged the X-ray events of grade 0 (single pixel), 2 (vertical 2-pixel split), 3 (leading horizontal 2-pixel split), 4 (trailing horizontal 2-pixel split), and 6 (L-shape or  $2 \times 2$ -pixel square shape) as valid X-ray events and those of grade 7 as invalid<sup>19</sup>. So, we reconstructed the X-ray events by the “fitting method”.<sup>20</sup> In the fitting method, we fit the elliptical distribution of charge on the CCD surface with a two dimensional non-spherical Gaussian function. we can make use of more spread events which are labeled as grade 7 and discarded when the grade method is used. Then we found the detection efficiency for X-rays from  $^{109}\text{Cd}$  (22.2 keV) is 11.8%, which is

equivalent to that of  $\sim 193 \mu\text{m}$  thickness of the depletion layer. This is essentially equal to the thickness of wafer ( $200\mu\text{m}$ ) and suggests this device is probably fully depleted.

Figure 7 shows the acquired image of  $\beta$ -ray with BI 15-22. BI 15-22 is essentially same as the BI 15-14 except that the surface of BI 15-22 is coated by the Al for the optical blocking. We irradiated the  $\beta$ -ray ( $^{90}\text{Sr}$ ) to the whole area of the CCD. The energy of the  $\beta$ -ray is 546 keV.  $\beta$ -ray interacts with silicon by the ionization loss and generates the electron-hole pairs along its track. Generated charges drift along the electric field in the depletion layer.

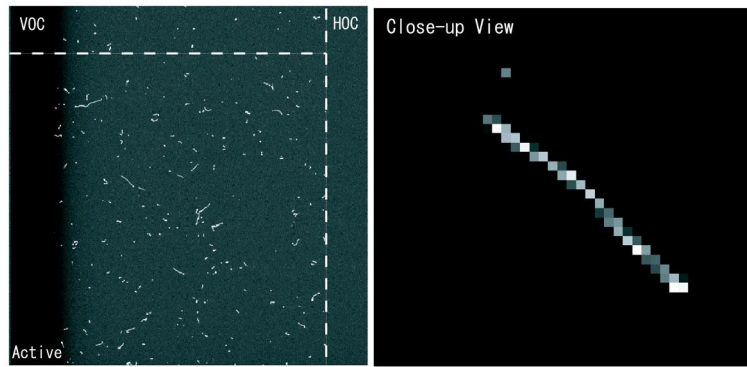


**Figure 7.** Image of  $\beta$ -ray from  $^{90}\text{Sr}$  detected by BI 15-22 with the back bias voltage of 5V. White dotted line shows the border between active and VOC, and HOC regions. We irradiated the  $\beta$ -ray ( $^{90}\text{Sr}$ ) to the whole area of the CCD.

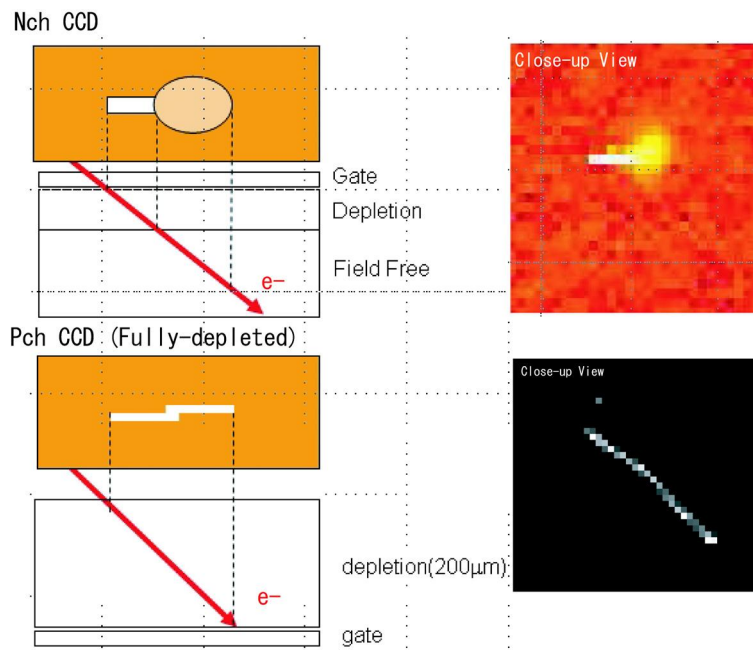


**Figure 8.** Schematic view of the interaction of  $\beta$ -ray in a CCD and the example of the image of  $\beta$ -ray track obtained by a CCD. (Upper) In the case of the typical Nch CCD. The image of  $\beta$ -ray track is obtained by CCD-CREST.<sup>21</sup> (lower) In the case of the fully-depleted CCD.

They make the unique charge distribution whether charges are generated in depletion layer or field-free region. We show the schematic view in Figure 8; When a  $\beta$ -ray interacts in the depletion layer, the created holes drift

rapidly to the gate electrode, so forming the narrow charge distribution of track as “tail”. On the other hand, when a  $\beta$ -ray interacts in the field-free layer, the created holes expand slowly by the diffusion process up to reach the depletion layer, so forming more wide charge distribution of track as “head”. Therefore, if the device is fully depleted, there is no  $\beta$ -ray events which has the “head” structure. As shown in Figure 7, we cannot see the  $\beta$ -ray events with “head”, so we can expect that almost the entire field-free region is removed.

### 3.4. $\beta$ -ray Image for various back bias voltages

Figure 9 shows the images of  $\beta$ -ray from  $^{90}\text{Sr}$  detected by BI 15-06 with the back bias voltage of 1, 5, 10, and 20V. The tracks of  $\beta$ -ray are seen more clearly and the charge distribution of tracks becomes narrower, as the voltage level of the back bias electrode increased. This suggests the size of the hall cloud is successfully restrained at the high back bias voltage level as we expected.

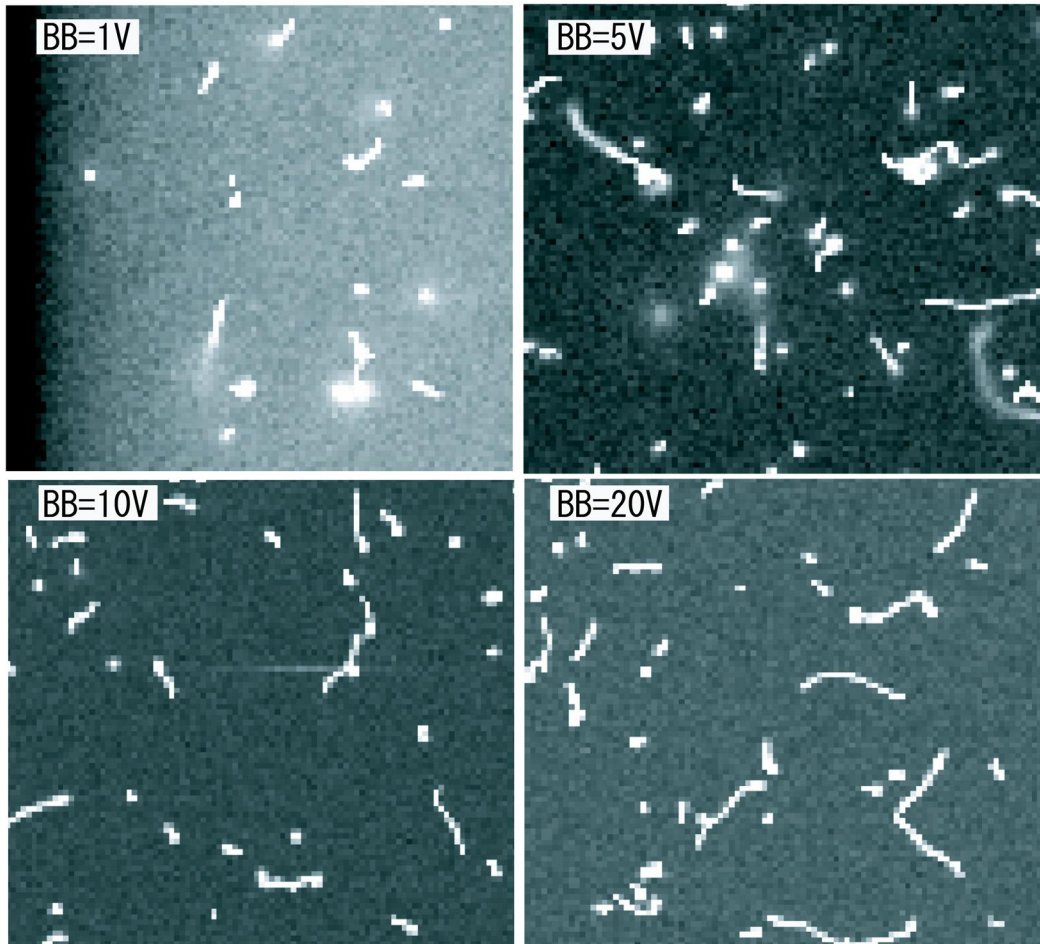


**Figure 9.** Images of  $\beta$ -ray from  $^{90}\text{Sr}$  detected by BI 15-06 with the back bias voltage of 1, 5, 10, and 20V. We irradiated the  $\beta$ -ray ( $^{90}\text{Sr}$ ) to the whole area of the CCD.



### 3.5. Optical blocking by Aluminum coating

As described previously, we coated the surface of BI 15-22 with Al to block the optical photons. We evaluated the efficiency of the optical blocking by the surface Al coating layer. We installed the red LED in the vacuum chamber. Comparing with the BI 15-14 which has no Al layer, we determined the optical transmissivity of BI 15-22. Figure 10 shows the comparison of dark images acquired by BI 15-22 and BI 15-14. We irradiated the LED light to BI 15-22 and BI 15-14 at the luminous time of 3 sec and 180 msec, respectively. The LED luminance is common in both cases. Nevertheless the luminous time is much longer than that for BI 15-14, we can clearly see a small amount of charges is generated in the active area of BI 15-22. This suggests the surface Al coating layer successfully blocks the optical light. The amount of generated charge per unit time in BI 15-22 and BI 15-14 were  $384 \text{ e}^-/\text{s}/\text{pixel}$  and  $1.2 \times 10^5 \text{ e}^-/\text{s}/\text{pixel}$ , respectively. Therefore, the transmissivity of the surface Al layer of BI 15-22 was estimated to be 0.32 %. We note that, however, the transmissivity is possibly overestimated. Since we irradiated LED to the whole area of CCD chip, CCD probably detected LED light incident from the side face of CCD chip which is not coated with Aluminum.

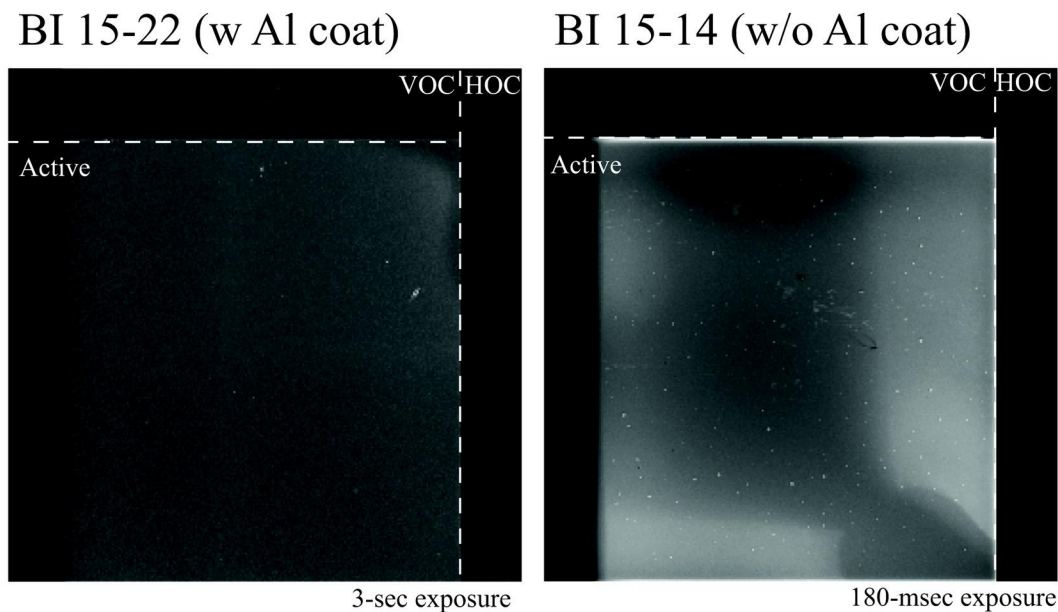


**Figure 10.** Comparison of images acquired by BI 15-22 and BI 15-14. We irradiated the LED light to BI 15-22 and BI 15-14 at the luminous time of 3 sec and 180 msec, respectively. The LED luminance is common in both cases. We can clearly see the Al layer coating the surface of BI 15-22 successfully blocks the optical light.

## 4. SUMMARY

We summarize the development of the back-illuminated and fully-depleted CCD for SXI following the goal plan;

- We fabricated the test devices of the fully-depleted and back-illuminated CCD on the high resistivity N-type wafer, which thinned down to  $200\mu\text{m}$ .
- We confirmed these devices successfully detected X-rays and were almost fully-depleted by the measurement of the detection efficiency for  $^{109}\text{Cd}$  and the shape of the  $\beta$ -ray track.
- We formed a back bias electrode on the backside surface of these test devices in order to intensify the electric field in a depletion layer. We confirmed there are not few changes in the spectroscopic performance dependent on the back bias voltage and the size of the hall cloud is successfully restrained at the high back bias voltage level from the image of the  $\beta$ -ray events.

- For optical blocking, we coated the surface of BI 15-22 with Aluminum. The measured transmissivity of this Aluminum layer is less than 0.32 %. This suggests the surface Al coating layer successfully blocks the optical light.

## ACKNOWLEDGMENTS

This work is supported by the Grant-in-Aid for the 21st Century COE "Center for Diversity and Universality in Physics" from the Ministry of Education, Culture, Sports, Science and Technology (MEXT) of Japan. S.T. was supported by JSPS Research Fellowship for Young Scientists.

## REFERENCES

1. Kunieda, H., Inoue, H., Mitsuda, K. and Takahashi, T., "New x-ray telescope mission (NeXT)", in *Proceedings of the SPIE, Volume 5488, pp. 187-196 (2004)*.
2. Y. Tawara, H. Kunieda, H. Inoue, K. Mitsuda, Y. Ogasaka, and T. Takahashi, "Broadband x-ray imaging mission NeXT," in *X-Ray and Gamma-Ray Telescopes and Instruments for Astronomy. Edited by Joachim E. Truemper, Harvey D. Tananbaum. Proceedings of the SPIE, Volume 4851, pp. 324-330 2003*.
3. Okajima, T., Tawara, Y., Ogasaka, Y., Tamura, K., Furuzawa, A., Yamashita, K., and Kunieda, H. "Hard X-ray focusing optics up to 80 keV for the future missions", in *Advances in Space Research, 34*, pp. 2682-2687 2004.
4. Takagi, S.-i. , Tsuru, T. G. , Matsumoto, H. , Koyama, K. , Tsunemi, H. , Miyata, E. , Miyazaki, S. , Kamata, Y. , Muramatsu, M. , Suzuki, H. and Miyaguchi, K., "Performance of back supportless CCDs for the NeXT mission", in *Nuclear Instruments and Methods in Physics Research A, 541*, pp. 385-391, 2005
5. T.G. Tsuru, S. Takagi, H. Matsumoto, T. Inui, K. Koyama, H. Tsunemi, K. Hayashida, E. Miyata, T. Dotani, M. Ozaki et al., "The development of a back-illuminated supportless CCD for SXI onboard the NeXT satellite", in *Nuclear Instruments and Methods in Physics Research A, 541*, pp. 392-397, 2005
6. T. Takahashi, K. Makishima, Y. Fukazawa, M. Kokubun, K. Nakazawa, M. Nomachi, H. Tajima, M. Tashiro, and Y. Terada, "Hard X-ray and  $\gamma$ -ray detectors for the NeXT mission," *New Astronomy Review 48*, pp. 269–273, Feb. 2004.
7. Nakajima, H. , Yamaguchi, H. , Matsumoto, H. , Tsuru, T. G. , Koyama, K. , Kissel, S. , LaMarr, B. and Bautz, M. "The ground calibration of X-ray CCD cameras (XIS) with front-illuminated chips onboard Astro-E2", in *Nuclear Instruments and Methods in Physics Research A, 541*, pp. 365-371, 2005
8. Takahashi, T., Nakazawa, K., Watanabe, S., Sato, G., Mitani, T., Tanaka, T., Oonuki, K., Tamura, K., Tajima, H., Kamae, T., Madejski, G., Nomachi, M., Fukazawa, Y., Makishima, K., Kokubun, M., Terada, Y., Kataoka, J. and Tashiro, M., "Application of CdTe for the NeXT mission", in *Nuclear Instruments and Methods in Physics Research A, 541*, pp. 332-341, 2005
9. Bamba, A., Kohno, M., Murakami, H., Imanishi, K., Tsujimoto, M., Tsuru, T., Koyama, K., Awaki, H., Kitamoto, S., Hayashida, K., Katayama, H. and Tsunemi, T. "Evaluations of Domestic X-ray CCDs with XIS Analog Electronics" in *Proceedings of New Century of X-ray Astronomy, ASP Conference Series, 251*, pp. 518, 2001
10. Tomida, H., Matsuoka, M., Torii, K., Ueno, S., Sugizaki, M., Yuan, W. M., Shirasaki, Y., Sakano, M., Komatsu, S., Tsunemi, H., Miyata, E., Kawai, N., Yoshida, A., Mihara, T. and Tanaka, I., "Solid state slit camera (SSC) of the MAXI mission for JEM (Japanese Experiment Module) on the International Space Station (ISS)", in *Proc. SPIE, X-Ray and Gamma-Ray Instrumentation for Astronomy XI, Kathryn A. Flanagan; Oswald H. Siegmund; Eds. 4140*, pp. 304–312, 2000
11. Miyata, E., Natsukari, C., Kamazuka, T., Akutsu, D., Kouno, H., Tsunemi, H., Matsuoka, M., Tomida, H., Ueno, S., Hamaguchi, K. and Tanaka, I. "Developments of engineering model of the X-ray CCD camera of the MAXI experiment onboard the International Space Station", in *Nuclear Instruments and Methods in Physics Research A, 488*, pp. 184–190, 2002
12. Ozawa, H., Tohiguchi, M., Matsuura, D., Miyata, E., Tsunemi, H., S. Takagi, T. Inui, T. G. Tsuru, Y. Kamata, H. Nakaya, S. Miyazaki, K. Miyaguchi, M. Muramatsu, H. Suzuki "Development of a p-type CCD for NeXT: the next Japanese X-ray astronomical satellite mission" in *Proceedings of the SPIE*, submitted

13. Groom, D. E., Holland, S. E., Levi, M. E., Palαιο, N. P., Perlmutter, S., Stover, R. J. and Wei, M., "Back-illuminated, fully-depleted CCD image sensors for use in optical and near-IR astronomy", in *Nuclear Instruments and Methods in Physics Research A*, **442**, pp. 216–222, 2000
14. Holland, A. D., "New developments in CCD and pixel arrays", in *Nuclear Instruments and Methods in Physics Research A*, **513**, pp. 308–312, 2003
15. Kamata, Y., Miyazaki, S., Muramatsu, M., Suzuki, H., Miyaguchi, K., Tsuru, T. G., Takagi, S.-i., Miyata, E., "Development of thick back-illuminated CCD to improve quantum efficiency in optical longer wavelength using high-resistivity n-type silicon", in *Optical and Infrared Detectors for Astronomy. Edited by James D. Garnett and James W. Beletic. Proceedings of the SPIE*, **5499**, pp. 210–218, 2004
16. Komiyama, Y., Miyazaki, S., Nakaya, H., Furusawa, H. and Takeshi, K., "Subaru next-generation wide-field camera: HyperSuprime", in *Ground-based Instrumentation for Astronomy. Edited by Alan F. M. Moorwood and Iye Masanori. Proceedings of the SPIE*, **5492**, pp. 523–532, 2004
17. Matsuura, D., Tohiguchi, M., Ozawa, H., Miyata, E., Tsunemi, H., S. Takagi, T. Inui, T. G. Tsuru, Y. Kamata, H. Nakaya, S. Miyazaki, K. Miyaguchi, M. Muramatsu, H. Suzuki "Development of N-type CCDs for NeXT, the next Japanese X-ray astronomical satellite mission" in *Proceedings of the SPIE*, submitted
18. E. Miyata, D. Kamiyama, H. Kouno, N. Nemesh, H. Tomida, H. Katayama, H. Tsunemi, and M. Matsuoka, "Flight CCD selection for the x-ray CCD camera of the Monitor of All-sky X-ray Image and mission onboard the International Space Station," in *X-Ray and Gamma-Ray Instrumentation for Astronomy XIII. Edited by Flanagan, Kathryn A.; Siegmund, Oswald H. W. Proceedings of the SPIE, Volume 5165, pp. 366-374 (2004).*, pp. 366–374, Feb. 2004.
19. NASA Research Announcement NRA 93-OSS-08.
20. Murakami, H. and Tsuru, T. G. and Awaki, H. and Sakano, M. and Nishiuchi, M. and Hamaguchi, K. and Koyama, K. and Tsunemi, H., "New event analysis method with the x-ray CCD camera XIS for ASTRO-E", in *Proc. SPIE, EUV, X-Ray, and Gamma-Ray Instrumentation for Astronomy X, Oswald H. Siegmund; Kathryn A. Flanagan; Eds.*, **3765**, pp. 160–170, 1999
21. M. Tsujimoto, Master Thesis, Kyoto University, 2000